Published in final edited form as:
Cell. 2014 June 5; 157(6): 1309–1323. doi:10.1016/j.cell.2014.03.062.

Cytotoxic cells kill intracellular bacteria through Granulysin-mediated delivery of Granzymes

Michael Walch[1,3,6,*], **Farokh Dotiwala**[1,6], **Sachin Mulik**[1], **Jerome Thiery**[1,4], **Tomas Kirchhausen**[1], **Carol Clayberger**[2], **Alan M. Krensky**[2], **Denis Martinvalet**[1,5], and **Judy Lieberman**[1,*]

[1]Program in Cellular and Molecular Medicine, Boston Children's Hospital, Harvard Medical School, 200 Longwood Avenue, Boston, MA 02115, USA

[2]Feinberg School of Medicine, Northwestern University, 420E Superior Street, Chicago, IL, 60611, USA

Summary

When killer lymphocytes recognize infected cells, perforin delivers cytotoxic proteases (granzymes) into the target cell to trigger apoptosis. What happens to intracellular bacteria during this process is unclear. Human, but not rodent, cytotoxic granules also contain granulysin, an antimicrobial peptide. Here we show that granulysin delivers granzymes into bacteria to kill diverse bacterial strains. In E. coli, granzymes cleave electron transport chain complex I and oxidative stress defense proteins, generating ROS that rapidly kill bacteria. ROS scavengers and bacterial antioxidant protein overexpression inhibit bacterial death. Bacteria overexpressing a GzmB-uncleavable mutant of the complex I subunit nuoF or strains that lack complex I still die, but more slowly, suggesting that granzymes disrupt multiple vital bacterial pathways. Mice expressing transgenic granulysin are better able to clear L. monocytogenes. Thus killer cells play an unexpected role in bacterial defense.

Introduction

Immune killer cells help control intracellular bacteria, such as listeria and mycobacteria, that evade other immune mechanisms by replicating within phagocytes. When killer cells recognize infected cells they release their cytotoxic granule contents into the immune synapse formed with the target cell to induce apoptosis (Chowdhury and Lieberman, 2008). Host cell apoptosis is triggered by the cytotoxic granule serine proteases (granzymes, Gzm),

*Correspondence should be addressed to J.L. (judy.lieberman@childrens.harvard.edu) or Michael Walch (michael.walch@unifr.ch).
[3]Present address: Department of Medicine, University of Fribourg, Route Albert Gockel 1, 1700 Fribourg, Switzerland
[4]Present address: INSERM U753, Institut Gustave Roussy-PR1, Rue Camille Desmoulins 39, 94805 Villejuif, France
[5]Present address: Centre Médical Universitaire, University of Geneva, Rue Michel-Servet 1, 1211 Geneva, Switzerland
[6]These authors contributed equally to this work.

Detailed methods are available online as Supplemental Information.

delivered into the target cell by the pore forming protein, perforin (PFN). The Gzms are not known to play any direct role in eliminating intracellular bacterial pathogens. There are 5 human Gzms that independently activate programmed host cell death, but GzmA and GzmB are the most abundant. GzmB activates the caspase pathway, while GzmA activates caspase-independent programmed cell death.

Cytotoxic granules of humans and some other mammals, but not rodents, also contain a saposin-like pore-forming protein, granulysin (GNLY), which preferentially disrupts cholesterol-poor bacterial, fungal and parasite membranes (Krensky and Clayberger, 2009; Stenger et al., 1998). Incubation of extracellular bacteria, including mycobacteria, with GNLY is cytolytic, but only using micromolar GNLY concentrations or extremely hypotonic or acidic buffers (Ernst et al., 2000; Stenger et al., 1998), suggesting that GNLY acts mostly against bacteria within acidic phagosomes or may act with other agents. GNLY and the Gzms, especially GzmB, are induced when T cells are incubated with bacteria (Walch et al., 2009). Patients with T cell immunodeficiency have increased susceptibility to bacterial, fungal and parasitic infections. These findings suggest that human T cells might control bacteria in unanticipated ways.

Mitochondria evolved from ancient bacterial symbionts within eukaryotic cells (Gray, 2012). In eukaryotic cells targeted for immune elimination, Gzms enter mitochondria where they cleave proteins in electron transport chain (ETC) complex I to generate superoxide anion, which plays a critical role in inducing apoptosis (Martinvalet et al., 2008). In fact, superoxide scavengers completely block cytolysis by killer lymphocytes (Martinvalet et al., 2005). The core proteins of electron transport in mammals derive from bacteria. Here we show that GNLY delivers Gzms into bacteria to trigger rapid bacterial death. In aerobic *E. coli*, as in mammalian cells, Gzms A and B cleave subunits of ETC complex I, generating superoxide anion. At the same time the Gzms cleave bacterial superoxide dismutases and catalases, enzymes that inactivate superoxide anion and peroxide, thus enhancing bacterial vulnerability to oxidative damage and promoting bacterial death. *E. coli* lacking ETC I or expressing a Gzm-resistant mutant of the key complex I substrate (NuoF) are still killed, but more slowly. Intracellular *Listeria monocytogenes* (*Lm*) are killed independently of the caspases and before the host cell in a process that depends on a Gzm, GNLY and PFN. Mice carrying a *GNLY* transgene (Tg) expressed only in killer lymphocytes (Huang et al., 2007) are more resistant to *Lm* infection than wild-type (WT) mice. The protective effect of GNLY is lost in $Prf1^{-/-}$ mice. Thus the Gzms, GNLY and PFN together kill intracellular bacteria.

Results

Gzms and sublytic GNLY induce rapid bacterial death

Gram- *E. coli* and gram+ *Lm* or *S. aureus* were treated with GzmA or B ± a sublytic concentration of GNLY (100-400 nM, depending on the preparation) that lyses <20% of bacteria (Figure S1). Bacterial viability was assessed by colony-forming assay (Figure 1A and 1B) and optical density (OD) measurement of bacterial growth (Figure 1C and 1D). Bacterial death was assessed by bacterial LIVE/DEAD® assay, which measures membrane integrity by relative uptake of Syto-9, which enters both live and dead cells, and propidium iodide (PI), taken up only by dead cells (Figure 1E-G). Bacterial viability and membrane

integrity were significantly reduced by just 5 min exposure to sublytic GNLY and either Gzm, but were not killed by proteolytically inactive Ser-Ala (S-A) Gzm (Figure 1A and 1B). Gzm/GNLY treatment shifted growth curves to the right by 200-400 min (Figure 1C). Given the bacterial doubling time of ∼30 min, these results suggest that >95% of bacteria were killed. To compare growth curves, the ratio of the time for untreated vs treated bacteria to grow to an OD of 0.05 was defined as the relative threshold time ($T_{threshold}$ (untreated/treated)) (Figure 1D). Because colony formation, growth curve quantitation and the cell death assay consistently gave comparable results, they were used interchangeably in this paper.

Sublytic GNLY delivers Gzms into bacteria

Since GNLY permeabilizes bacterial cell membranes (Ernst et al., 2000), we hypothesized that GNLY might deliver Gzms into bacteria. Confocal microscopy (Figure 2A-D, Supplementary Movies 1-6) of *E. coli* treated with fluorescently labeled (AlexaFluor (AF)-488) Gzms with and without GNLY showed that Gzms were internalized into bacteria in a GNLY-dependent manner. In bacteria treated with AF-488 GzmB and AF-647 GNLY, GzmB entered bacteria, while GNLY stayed on the surface (Figure 2B). GzmB internalization was quantified (Figure 2D) by counting the number of cells clearly showing intracellular fluorescence, assessing at least 300 bacteria per condition. GzmB uptake was confirmed by flow cytometry (Figure 2E). Thus GNLY delivered Gzms into bacteria.

Intracellular *Lm* are killed in a Gzm, GNLY and PFN-dependent process

To test GzmB activity against intracellular bacteria, *Lm*-infected HeLa cells were treated with combinations of GzmB, PFN and GNLY (Figure 3A). After 1 hr, we measured host cell death by annexin V and PI staining and viable *Lm* colonies (CFU) from hypotonically lysed cells. Host cell killing required both GzmB and PFN and was not enhanced by GNLY. PFN and GzmB without GNLY did not significantly affect *Lm* viability, suggesting that host cell death does not kill intracellular bacteria. Fewer bacterial colonies grew in cells treated with GNLY and either PFN or GzmB. However, bacterial viability was most reduced when all 3 effector molecules were applied. We repeated this experiment using HeLa cells stably overexpressing *BCL2*, which inhibits GzmB-mediated apoptosis. *BCL2* overexpression rescued host cells, but did not affect *Lm* CFUs (Figure S2A). Host cells were killed independently of GNLY, but required both PFN and GzmB, while efficient bacterial elimination required all 3 enzymes. This result is consistent with a previous report showing that host cell apoptosis is neither sufficient nor necessary for $CD8^+$ CTL to kill intracellular *M. tuberculosis* (Thoma-Uszynski et al., 2000).

A human *Lm*-specific CD8 T cell line was used to test whether CTLs destroy intracellular *Lm* in infected monocyte-derived dendritic cells (MDDC). Incubation of infected MDDC for 2 hr with increasing numbers of killer cells reduced both host cell and *Lm* viability compared to cultures without CTLs (Figure 3B). Bacteria were killed at lower effector:target cell (E:T) ratios than host cells. Bacterial viability was significantly reduced after 30 min, but host cell death, measured by ^{51}Cr release, did not become significant until 90 min after adding killer cells (Figure 3C). Thus intracellular *Lm* killing was more efficient and rapid than host cell killing. Rapid bacterial destruction before host cell lysis could reduce

pathogen spreading from dying cells. Caspase inhibition reduced host cell death, but bacterial death was unaffected, confirming the independence of bacterial and host cell death (Figure 3B). Both deaths were completely inhibited by the Gzm inhibitor, 3,4-dichloroisocoumarin (DCI) (Figure 3B). Thus bacterial death requires active Gzms and does not depend on activated caspases or host cell death.

To assess the importance of GNLY in bacterial elimination by mouse killer lymphocytes, we compared splenocytes from *GNLY*-transgenic (Tg, *GNLY* $^{-/+}$) and wild-type (WT) BALB/c mice (Huang et al., 2007). The Tg was only expressed in CTL and natural killer (NK) cells, like the endogenous human protein (Figure S2B). In the spleens of naïve *GNLY*-Tg mice, GNLY was expressed by about a third of NKp46^{+} NK cells, but was not expressed by T or B cells or myeloid cells. After 5 d of *in vitro* IL-2, about two-thirds of NK cells and a third of CD8 T cells, but only 7% of CD4 T cells, from *GNLY*-Tg mice expressed GNLY (Figure 3D and S2C). GzmB expression was comparable in WT and *GNLY*-Tg mice. After in vitro culture in IL-15, GNLY was only expressed in NK cells and CD62L^{-}CD44^{+} effector and effector memory CD8 T cells from Tg mice (Figure S2C).

To assess the role of Gzms and PFN in GNLY-mediated bacterial killing, *GNLY*-Tg mice were backcrossed with *Gzmb*$^{-/-}$ and *Prf1*$^{-/-}$ BALB/c mice. Splenocytes from each strain, harvested 8 days after *Lm* infection, were incubated with anti-CD3-coated *Lm*-infected RAW264.7 cells (Figure 3E). WT and *Gzmb*$^{-/-}$ splenocytes killed host cells and *Lm* equivalently, probably because the lack of GzmB is well compensated by other Gzms (Chowdhury and Lieberman, 2008). PFN-deficient splenocytes, even if they expressed *GNLY*, did not kill host cells or intracellular bacteria. The *GNLY*-Tg had no significant effect on host cell killing, but significantly reduced bacterial survival. PFN-sufficient killer cells reduced *Lm* CFUs even in the absence of the Tg, presumably because a dying cell is not a hospitable host. Thus, rapid, efficient bacterial death requires both GNLY and PFN.

GNLY-Tg mice clear *Lm* more effectively than WT mice

To examine the *in vivo* significance of GNLY-mediated destruction of intracellular bacteria, we assessed the effect of the *GNLY*-Tg in WT, *Gzmb*$^{-/-}$ and *Prf1*$^{-/-}$ backgrounds on clearance of intraperitoneally injected *Lm* (0.2 LD_{50}) (Figure 3F). *GNLY*-Tg mice that expressed PFN more effectively cleared *Lm*. Bacterial counts in the liver and spleen 3 d later were reduced by ∼3 logs in *GNLY*-Tg WT and *Gzmb*$^{-/-}$ mice. As expected (Kagi et al., 1994), PFN-deficient mice had significantly more *Lm* in the spleen and a trend towards increased bacteria in the liver than WT and *Gzmb*$^{-/-}$ mice, and the *GNLY*-Tg provided no protection. Thus GNLY antibacterial activity in naïve mice requires PFN, implicating the granule exocytosis pathway of innate cytotoxic effector cells in antibacterial immune defense. The more efficient clearance by *GNLY*-Tg naïve mice was likely due to NK cells, since these are the only cells that express GNLY in naïve mice (Figure S2; (Huang et al., 2007)).

While NK cells protect naïve mice from *Lm*, CD8 T cells are the mainstays of immune protection in previously exposed mice. To assess the importance of GNLY in CD8 T cells in the recall response, WT and *GNLY*-Tg mice in *Prf1* WT or deficient backgrounds were immunized with 0.2 LD_{50} *Lm* and 3 weeks later challenged with 20 LD_{50} (Figure 3G). 2 of 8 *GNLY*$^{+/-}$*Prf1*$^{+/+}$ mice completely cleared *Lm* within 40 hr, while all WT mice had

detectable bacteria. Moreover, *GNLY*-Tg mice that had detectable bacteria had on average ∼3 logs fewer bacteria than WT mice. As in the primary response, the *GNLY* Tg provided no advantage in PFN-deficient mice, indicating that PFN is needed for both NK cells and T cells to kill intracellular bacteria.

GNLY-delivered Gzms rapidly induce ROS in bacteria

An early event in Gzm-induced death of mammalian cells is ROS induction (Martinvalet et al., 2008). Neutrophils and macrophages rely on ROS to kill phagocytosed bacteria (Hampton et al., 1998). Bactericidal antibiotics may also elicit ROS to kill bacteria efficiently, although this finding has been recently contested (Kohanski et al., 2007; Keren et al., 2013; Liu and Imlay, 2013). A schematic of ROS pathways in bacteria is shown in Figure 4A. To assess whether GNLY-delivered GzmB induces ROS, bacteria were labeled with the superoxide-sensitive fluorescent reporter, dihydroethidium (DHE). GzmB treatment of *E. coli*, *Lm* and *S. aureus* generated ROS in a GNLY and dose-dependent manner (Figure 4B). DHE staining showed both low and high fluorescence intensity populations, the latter increasing with Gzm concentration. (Since GNLY does not bind homogenously (Figure 2B), a lethal Gzm concentration may not accumulate in all cells at limiting Gzm concentrations, accounting for the nonfluorescent population.) ROS induction was detected within 5 min (Figure 4C). The superoxide-specific oxidation product of DHE, 2-hydroxyethidium (emission peak, ∼580 nm) can be distinguished from its nonspecific oxidation product, ethidium (605 nm) after excitation at 488 nm (Zhao et al., 2003) (Figure 4D and S3). H_2O_2 treatment generated only the ethidium peak. When *E. coli* were treated with GzmB/GNLY or the electron transport chain (ETC) complex I inhibitor rotenone, which induces superoxide, DHE-stained cells emitted at both wavelengths, suggesting that superoxide and other ROS were produced. To confirm H_2O_2 production, we measured its release from the catalase/peroxidase-null LC106 strain (Liu and Imlay, 2013) after treatment with GNLY/GzmB or the superoxide-inducing poisons, rotenone or paraquat (Figure 4E). As expected, treatment with either the poisons or GNLY/GzmB, but not GNLY or GzmB alone, significantly increased H_2O_2 production, which was inhibited by the superoxide scavenger Tiron or the H_2O_2 scavenger dimethylthiourea (DMTU). Complete inhibition by Tiron suggests that superoxide anion is the first ROS species formed.

E. coli sense and combat oxidative stress by activating the ROS sensors OxyR and SoxR, which preferentially sense H_2O_2 and superoxide, respectively, to trigger the rapid transcription of oxidative stress response genes (Chiang and Schellhorn, 2012). OxyR induces catalase (*katG*), ferrochelatase (*hemH*), and the regulatory RNA *oxyS* and represses *oxyR* itself in a negative feedback loop. SoxR oxidation induces transcription of *soxS*, which then drives expression of genes that protect against superoxide stress. Treatment of *E. coli* for 10 min with GzmB/GNLY, H_2O_2 or rotenone induced transcription of *soxS*, *oxyS*, *katG* and *hemH*, but not *oxyR* (Figure 4F). Tiron abolished the transcriptional response to GNLY/GzmB and rotenone, but had less of an effect on H_2O_2-treated cells, providing further evidence that GzmB/GNLY, like rotenone, induce the bacterial oxidative stress transcriptional program. *recA* deficient strains, impaired in DNA repair, are especially susceptible to ROS (Konola et al., 2000). As expected, *recA* mutants were significantly more susceptible to Gzm/GNLY killing (Figure 4G). These data taken together indicate that

superoxide and peroxide and other downstream ROS are rapidly generated in bacteria treated with GzmB and GNLY.

ROS contribute to rapid bacterial death induced by the Gzms

To assess whether superoxide anion and/or other ROS mediate bacterial death by GzmB/GNLY, we examined the effect of GNLY ± GzmB and the superoxide anion-inducers, rotenone and paraquat, as controls, on growth of *E. coli* overexpressing superoxide dismutase (*sodA*), which converts superoxide anion to H_2O_2, or catalase (*katG*), which inactivates H_2O_2. Overexpression of either oxidative defense enzyme protected bacteria from GzmB/GNLY (Figure 5A), suggesting that superoxide and its downstream product H_2O_2 both contributed to the toxic effect of GzmB and GNLY. As expected, overexpressing *sodA* protected against paraquat, but not H_2O_2, while *katG* provided protection against H_2O_2 (Figure 5A). Rotenone and paraquat at the concentrations used induced similar levels of H_2O_2 as GzmB and GNLY (Figure 4E). However, although these strong oxidants inhibited bacterial growth, because of effective antioxidant defenses, bacteria survived treatment with paraquat and H_2O_2, as assessed by the LIVE/DEAD assay (Figure 5B). However, GzmB and GNLY not only caused growth arrest, but also induced death. This death was largely rescued by *sodA* overexpression, which also greatly reduced superoxide levels as monitored by DHE fluorescence (Figure 5C), suggesting that superoxide generation plays a critical role in initiating bacterial death. Since bacteria are able to recover from strong oxidative stresses that generate comparable levels of peroxide, but die from Gzm and GNLY treatment, it is likely that GzmB does more than generate ROS (see below).

Tiron and Mn(III)tetrakis(4-benzoic acid)porphyrin (MnTBAP), which act as superoxide reducing agents (Ledenev et al., 1986) or inhibit superoxide formation (Taiwo, 2008), completely blocked rapid bacterial death (Figure 5D). Trolox, an α-tocopherol derivative that scavenges free radicals, the hydrogen peroxide scavenger DMTU and the iron-chelator deferoxamine also reduced bacteria killing, but less than Tiron or MnTBAP, providing further evidence that superoxide anion is the first ROS species produced. Superoxide damages Fe-S cluster-containing enzymes, such as aconitase (Gardner and Fridovich, 1991). To confirm that superoxide was generated by GNLY and GzmB, we measured aconitase activity in treated *E. coli*. GzmB and GNLY, but not GNLY on its own, rapidly reduced aconitase activity to a similar extent as rotenone (Figure 5E). Moreover, Tiron, which enhanced aconitase activity of untreated bacteria, completely rescued aconitase activity after GzmB/GNLY or rotenone treatment. Thus superoxide anion initiates bacterial death that is executed in part by downstream ROS.

Gzm cleavage of bacterial complex I subunits causes oxidative damage

GzmA and GzmB generate ROS in mammalian cells by cleaving ETC complex I (Martinvalet et al., 2008; Jacquemin et al., submitted). The core components of electron transport are conserved between bacteria and mammals. Bacterial complex I (a simpler enzyme of 13 or 14 subunits in bacteria versus 45 in mammals (Efremov et al., 2010; Spehr et al., 1999)) is an L-shaped complex with one arm embedded in the membrane (NADH-ubiquinone-oxidoreductase (Nuo) subunits A, H, J-N), connected by a cytosolic stalk (subunits B, CD, I) to the catalytic core (subunits E, F, G, see Figure 7C) (Efremov et al.,

2010). Incubation of purified *E. coli* complex I with nM concentrations of GzmA or GzmB for 10 min led to cleavage of several Nuo subunits, as visualized by Coomassie blue staining (Figure 6A). NuoF, the homolog of mammalian NDUFV1, which binds NADH to initiate electron transport (Friedrich and Weiss, 1997), was the best substrate. Bands for NuoG, NuoCD (both in the catalytic domain (Efremov et al., 2010)) and possibly NuoL and NuoM also were reduced in intensity at the highest concentration (200 nM). GzmA (70 nM) cleaved NuoF and NuoG comparably, generating an ∼80 kDa NuoG cleavage product. To verify their cleavage, since no antibodies were available, the NuoG, NuoCD, NuoF and NuoM candidate substrates were expressed as N-terminal GST-fusion proteins in *E. coli* and purified for *in vitro* Gzm cleavage assays (Figure S4A) or tested for cleavage in intact bacteria (Figure 6B and C). NuoCD, F and G were *in vitro* substrates of both GzmA and GzmB with detectable cleavage products, which were analyzed by mass spectrometry to determine their cleavage sites. NuoM was not a substrate. Thus the Gzms target the more accessible, catalytic components of complex I. GzmB cleaved NuoCD at D146, NuoF at D20, D27 and D48 and NuoG at D824. Although GzmA cleaved all 3 proteins, only the cleavage site of NuoCD was mapped (R228). These cleavage sites are consistent with the substrate specificity of GzmB for aspartic acid and the tryptase activity of GzmA. In bacteria expressing the fusion proteins, GzmB and GNLY treatment generated cleavage products of the 3 substrates, but not NuoM, detected by GST immunoblot, confirming that they are substrates in intact bacteria (Figure 6B). Four unrelated control *E. coli* proteins (XerC, MinC, NlpL, MotB), expressed as GST fusion-proteins, were not cleaved in GNLY and GzmB-treated *E. coli* (Figure S4B). The NuoCD cleavage fragment was detected within 5 min of GzmB treatment (Figure 6C), consistent with the timing of ROS production and bacterial death. Thus multiple cytosolic subunits of complex I are specific Gzm substrates in *E. coli*.

To determine whether NuoF cleavage contributes to ROS generation and bacterial death, a GzmB-uncleavable mutant of *E. coli* NuoF was generated by mutating the 3 cleavage site Asps to Ala (Figure S4C). GzmB and GNLY did not cleave triple mutant NuoF in bacteria, but GzmA cleavage was unaffected. ROS and death induced by GzmB and GNLY were significantly reduced and delayed in bacteria expressing triple mutant, compared to wild-type (WT), NuoF (Figure 6D and E). The mutation did not inhibit the effectiveness of GzmA. The importance of targeting complex I was also assessed using the *E. coli* strain, ANN0221/*pBADnuo/His-nuoF* (Figure 6F, S4D and S4E), in which an L-arabinose-sensitive promoter controls the *nuo* operon. These bacteria express His-tagged NuoF (Spehr et al., 1999), only when L-arabinose is in the medium (Figure S4D). Lack of complex I completely protected GzmB and GNLY-treated bacteria from ROS induction and rapid death, measured after 15 min. However, after 1 hr, viability of complex I-deficient bacteria was significantly reduced, although ROS measured by DHE fluorescence only increased slightly. Thus GzmB kills bacteria independently of complex I, although with delayed kinetics. To confirm that ETC complex I is the source of superoxide, we compared superoxide/peroxide generation by GzmB-treated membranes prepared from arabinose-induced or uninduced ANN0221/*pBADnuo/His-nuoF* bacteria by measuring NADH oxidation and cytochrome c reduction (Figure S4D). Complex I sufficient membranes generated superoxide in response to GzmB and rotenone, but deficient membranes did not.

We compared the rate of NADH oxidation with the rate of cytochrome c reduction in GzmB-treated and untreated membranes to estimate what proportion of electrons were channeled into superoxide production. In GzmB-treated membranes ~10% of electrons were channeled into superoxide, compared to only ~1% of electrons in untreated membranes. Addition of SOD to the reaction decreased cytochrome c reduction to background, confirming that superoxide anion was responsible (Figure S4E).

Complex I is poorly characterized in *Lm*. A BLAST search identified propanediol utilization protein, subunit S (PduS) as the best match for *E. coli* NuoF. *Lm pduS* contains the N-terminal NADH:ubiquinone oxidoreductase catalytic site sequence of mammalian NDUFV1, the key residues responsible for flavin mononucleotide binding and conserved cysteines that participate in the N3 Fe-S cluster. PduS was also a GzmB target, both in vitro and in *Lm* expressing the tagged protein (data not shown). Thus the Gzms may target oxidoreductases in diverse bacterial strains.

GzmB destroys ROS degrading enzymes in *E. coli*

The level of cellular ROS reflects the balance between ROS generation and elimination by cellular antioxidant defenses. Because GzmB/GNLY more effectively killed bacteria than paraquat (Figure 5B), we suspected that GzmB might also cleave and disable proteins that protect bacteria from oxidative damage. Indeed SodA and KatG GST fusion proteins were cleaved within 20 min in bacteria treated with GzmB/GNLY, but not GNLY on its own (Figure 7A). Furthermore, *in vitro* treatment of these purified enzymes with 150 nM GzmB decreased their catalytic activity (Figure 7B). Preliminary proteomics analysis suggests that GzmB cripples oxidative stress defense by cleaving all three Sods (A, B and C) and the major peroxide inactivating enzymes KatG, KatE and AhpC in *E. coli* (Seaver and Imlay, 2001). Thus ROS accumulates in GNLY/GzmB treated bacteria not only because superoxide is induced, but also because bacteria are less able to inactivate it.

Discussion

We propose a model in which first PFN delivers Gzms and GNLY into infected cells targeted for immune elimination and then GNLY introduces Gzms into bacteria (Figure 7C). In the bacterial cytosol Gzms proteolytically attack ETC complex I. Aerobic bacteria have powerful antioxidant responses, which enable them to withstand basal ROS generated in an aerobic environment and exposure to potent oxidants, such as paraquat and peroxide (Figure 5B). But the Gzms also cleave and inactivate the cornerstone enzymes of oxidative defense, the Sods and catalases. By crippling the oxidative stress response, the Gzms inflict irreparable damage.

Gzms and caspases induce apoptosis in mammalian cells by triggering programs targeting critical processes needed for survival - causing DNA damage, inducing ROS, disrupting the mitochondrial outer membrane, interfering with RNA splicing and protein translation. No one substrate/pathway is universally essential for death. For example mitochondrial damage is needed in some death pathways to kill some cells, but not others. DNA damage is not essential, since enucleated cells also undergo programmed cell death. Apoptosis also disrupts cellular repair, for example by cleaving and inactivating key DNA repair enzymes.

This multipronged attack means that virus-infected or cancer cells that resist damage to one pathway or another are still killed. The Gzms or caspases typically cleave a few hundred substrates in mammalian cells. Our data suggest that Gzm-mediated bacterial cell death is also a complex program of damage that disrupts key pathways and interferes with repair, providing a mechanism to kill diverse bacterial strains growing under varied conditions. A case in point is the death of bacteria lacking complex I, which suggests that both aerobic and anerobic bacteria will be killed. Preliminary proteomics analysis of GzmB-treated *E. coli* and *Lm* (not shown) suggests that the Gzms cleave ∼100-200 proteins in each species, many of which are functional homologues. GzmB is not indiscriminate in its targets. More than 90% of proteins are not substrates, and the candidate substrates are concentrated in pathways involved in aerobic and anerobic metabolism, DNA repair, protein synthesis and stress responses. Cleavage of other substrates will likely enhance the cytotoxic effect of Gzms against aerobes and lead to slower killing of anaerobes, broadening the impact of this immune defense mechanism. The implication is that it will be difficult for bacteria to evade or develop resistance to killer cell-mediated death. However, these putative additional substrates require careful experimental validation, and the effect of the Gzms on anaerobic bacteria and other bacterial strains requires further study.

Attack of complex I is a shared critical feature of programmed cell death in bacteria and mammalian cells (Martinvalet et al., 2008; Ricci et al., 2004). Superoxide scavengers protect against death in both systems. Cleavage of catalytic domains of complex I, which protrude into the cytosol of bacteria or the mitochondrial matrix of mammalian cells, disrupts the flow of electrons. In bacteria the dominant GzmA and B substrate NuoF, which binds NADH and FMN, initiates electron transport. Cleavage of NuoF at its N-terminal Asp residues D20, D27 and D48 by GzmB is not expected to disrupt electron capture at the NADH binding site (E95). We propose that electrons captured from NADH by complex I that are normally transferred to ubiquinone get sidetracked to react with dissolved oxygen to generate superoxide anion. Superoxide is not ordinarily cytotoxic for bacteria. Based on our experiments with ROS scavengers, catalase overexpression and measurement of H_2O_2 production, we propose that superoxide anion is rapidly converted to more cytotoxic intermediates, including peroxide. Moreover, proteolysis of SodA and KatG (and probably other oxidative repair enzymes) cripples bacterial handling of ROS to guarantee bacterial death. It will be worthwhile to examine whether the Gzms or caspases also cleave mammalian oxidative defense enzymes, which has not been studied.

Although we mostly focused on GzmB, preliminary data suggest that GzmA, as well as GzmM, an important Gzm in NK cells, also attack bacterial complex I. Myeloid cell serine proteases are also implicated in antibacterial defense. Mice deficient in neutrophil elastase or cathepsin G, which are closely related to the Gzms, are more susceptible to bacterial infection (Hirche et al., 2008; Steinwede et al., 2012). Neutrophils and other cells also express antimicrobial peptides with properties similar to GNLY (Gallo and Nizet, 2003). Other leukocyte serine proteases and antimicrobial peptides might substitute for Gzms and GNLY in bacterial defense.

Future experiments in *GNLY*-Tg mice should investigate whether Gzms and GNLY protect *in vivo* against extracellular bacteria. Gzm concentrations in extracellular fluids during

bacterial infection are unknown. Extracellular Gzms are elevated during viral infection and inflammation (such as in rheumatoid arthritic joints, in bronchoalveolar fluid of asthma patients, or in the blood during acute CMV or chronic HIV infection) (Spaeny-Dekking et al., 1998). GNLY has been measured in the plasma of healthy and tuberculosis-infected people (Pitabut et al., 2011). Gzm and GNLY concentrations in these settings were at most in the low-nanomolar range, below the concentrations we needed to kill extracellular bacteria *in vitro*. However, local concentrations may be higher at the site of infection, depending on the density and activation of infiltrating cytotoxic immune cells.

Heretofore, the main anti-infective function of killer lymphocytes in infection was thought to be antiviral. This study shows that NK cells and CTLs also protect us against intracellular bacteria by a novel mechanism that deploys all 3 classes of effector molecules, Gzms, GNLY and PFN. GNLY is active against cholesterol-poor membranes, found in bacteria, fungi and parasites, and the core components of electron transport are conserved amongst species. Thus the Gzm-PFN-GNLY trio may well act on other intracellular pathogens, including fungi and parasites. This merits further study.

Experimental Procedures

Treatment of bacteria with cytotoxic proteins

Gzms ± sublytic GNLY were incubated at 37°C with 10^5/ml exponential phase bacteria in 20 μl of 10 mM NaCl, 20 mM Tris (pH 7.4). A sublytic concentration of GNLY was chosen to cause <20% death by CFU assay. Treated bacteria were diluted in LB and plated on LB (*E. coli*, *S. aureus*) or BHI (*Lm*) agar plates to determine CFU, which were normalized to CFU in control conditions.

Imaging GzmB delivery

E. coli, treated with 500 nM AF488-labeled Gzm ± sublytic unlabeled or AF647-labeled $GNLY_{peptide}$ for 20 min at 37°C, were washed with 10 mM arginine in PBS for 10 min and stained with DAPI and in some cases FM4-64. Cells were fixed with 2% formalin in PBS and imaged by confocal microscopy.

Mouse strains

GNLY$^{+/-}$ BALB/c mice, originally described in (Huang et al., 2007), were rederived at Jackson Laboratory, and backcrossed for over 7 generations into BALB/c WT mice. These were bred with *Prf1*$^{-/-}$ (Jackson laboratory) and *Gzmb*$^{-/-}$ BALB/c mice (kind gift of T. Ley). Experiments were performed using 6–9 wk old mice. Animal use was approved by the Animal Care and Use Committees of Boston Children's Hospital and Harvard Medical School.

Measurements of intracellular bacterial and host cell killing

Lm-infected HeLa cells, detached by gentle trypsinization and resuspended in 10 mM HEPES, 4 mM $CaCl_2$, 0.4% BSA in HBSS at 10^6 cells/ml, were treated with GzmB, GNLY and sublytic PFN (pre-diluted in 10 mM HEPES in HBSS) at 37°C. Host cell viability was assessed by annexinV/PI staining and flow cytometry or ^{51}Cr release assay as described

(Thiery et al., 2010). Bacterial viability was measured by CFU after hypotonic lysis of host cells. For some experiments, HeLa cells stably overexpressing *BCL2* or empty vector were used.

For human CTL experiments, CD8-enriched *Lm*-specific T cells were added at indicated E:T ratios and times to infected MDDC. In some experiments T cells were preincubated with 250 μM DCI or PBS for 30 min at 37°C and washed with PBS. In some experiments, zVAD-fmk (75 μM) or DMSO (0.75%) was added during the killing assay. For mouse T cell experiments, *Lm*-infected RAW 264.7 target cells (MOI=5) were incubated for 10 min in medium containing 5 μg/ml anti-mouse CD3ε (clone 145-2C11, eBioscience). Splenocytes, obtained from mice infected with *Lm* 8 d earlier, were added at an E:T ratio of 3 for indicated times. Bacterial viability was measured by CFU as above. Host cell viability was assessed by ^{51}Cr release assay as described (Thiery et al., 2010).

In vivo anti-*Lm* activity

Freshly grown, exponential phase *Lm* (0.2 LD_{50}) were injected i.p. in 0.5 ml PBS. For the primary response, liver and spleen were harvested 72 h post-infection. For the recall response, immune mice were reinfected with 20 LD_{50} 3 wk later and organs were harvested after 40 h. Organs were weighed and homogenized in water with 0.2% Triton X-100. Colonies were counted after plating 10-fold serial dilutions on BHI agar.

Gzm cleavage assays

E. coli harboring GST-fusion protein expression plasmids were induced for 15 min at 37°C with 0.1 mM IPTG in LB containing 100 μg ampicillin and 2% glucose, washed and resuspended in 20 mM NaCl, 10 mM Tris, pH 7.4 before adding Gzms and sublytic GNLY. Reactions were stopped by boiling in SDS-PAGE loading buffer. Samples were analyzed by immunoblot using anti-GST goat polyclonal Ab (Pharmacia).

Supplementary Material

Refer to Web version on PubMed Central for supplementary material.

Acknowledgments

This work was supported by NIH AI-045587 (JL), the Stiefel-Zangger Foundation (MW) and PCMM-Glaxo Smith Kline Alliance (FD). We thank Zhan Xu and Solange Kharoubi Hess for technical support, Luis Filgueira for helpful discussions, Marshall Thomas for HeLa-BCL2 cells, James Imlay (University of Illinois) for valuable suggestions and for the L106 *E. coli* strain, Susan Lovett (Brandeis) for the *recA* strain, Thorsten Friedrich (Albert-Ludwigs-University, Freiburg, Germany) for *E. coli* strain ANN0221/*pBADnuo/His-nuoF*, and Darren Higgins (Harvard Medical School) for the *Lm* expression plasmid pLIV1.

References

Chiang SM, Schellhorn HE. Regulators of oxidative stress response genes in Escherichia coli and their functional conservation in bacteria. Arch Biochem Biophys. 2012; 525:161–169. [PubMed: 22381957]

Chowdhury D, Lieberman J. Death by a thousand cuts: granzyme pathways of programmed cell death. Annu Rev Immunol. 2008; 26:389–420. [PubMed: 18304003]

Efremov RG, Baradaran R, Sazanov LA. The architecture of respiratory complex I. Nature. 2010; 465:441–445. [PubMed: 20505720]

Ernst WA, Thoma-Uszynski S, Teitelbaum R, Ko C, Hanson DA, Clayberger C, Krensky AM, Leippe M, Bloom BR, Ganz T, et al. Granulysin, a T cell product, kills bacteria by altering membrane permeability. J Immunol. 2000; 165:7102–7108. [PubMed: 11120840]

Friedrich T, Weiss H. Modular evolution of the respiratory NADH:ubiquinone oxidoreductase and the origin of its modules. J Theor Biol. 1997; 187:529–540. [PubMed: 9299297]

Gallo RL, Nizet V. Endogenous production of antimicrobial peptides in innate immunity and human disease. Curr Allergy Asthma Rep. 2003; 3:402–409. [PubMed: 12906776]

Gardner PR, Fridovich I. Superoxide sensitivity of the Escherichia coli aconitase. J Biol Chem. 1991; 266:19328–19333. [PubMed: 1655783]

Gray MW. Mitochondrial evolution. Cold Spring Harbor Perspect Biol. 2012; 4:a011403.

Hampton MB, Kettle AJ, Winterbourn CC. Inside the neutrophil phagosome: oxidants, myeloperoxidase, and bacterial killing. Blood. 1998; 92:3007–3017. [PubMed: 9787133]

Hirche TO, Benabid R, Deslee G, Gangloff S, Achilefu S, Guenounou M, Lebargy F, Hancock RE, Belaaouaj A. Neutrophil elastase mediates innate host protection against Pseudomonas aeruginosa. J Immunol. 2008; 181:4945–4954. [PubMed: 18802098]

Huang LP, Lyu SC, Clayberger C, Krensky AM. Granulysin-mediated tumor rejection in transgenic mice. J Immunol. 2007; 178:77–84. [PubMed: 17182542]

Kagi D, Ledermann B, Burki K, Hengartner H, Zinkernagel RM. CD8+ T cell-mediated protection against an intracellular bacterium by perforin-dependent cytotoxicity. Eur J Immunol. 1994; 24:3068–3072. [PubMed: 7805735]

Keren I, Wu Y, Inocencio J, Mulcahy LR, Lewis K. Killing by bactericidal antibiotics does not depend on reactive oxygen species. Science. 2013; 339:1213–1216. [PubMed: 23471410]

Kohanski MA, Dwyer DJ, Hayete B, Lawrence CA, Collins JJ. A common mechanism of cellular death induced by bactericidal antibiotics. Cell. 2007; 130:797–810. [PubMed: 17803904]

Konola JT, Sargent KE, Gow JB. Efficient repair of hydrogen peroxide-induced DNA damage by Escherichia coli requires SOS induction of RecA and RuvA proteins. Mut Res. 2000; 459:187–194. [PubMed: 10812330]

Krensky AM, Clayberger C. Biology and clinical relevance of granulysin. Tissue Antigens. 2009; 73:193–198. [PubMed: 19254247]

Ledenev AN, Konstantinov AA, Popova E, Ruuge EK. A simple assay of the superoxide generation rate with Tiron as an EPR-visible radical scavenger. Biochem Int. 1986; 13:391–396. [PubMed: 3021163]

Liu Y, Imlay JA. Cell death from antibiotics without the involvement of reactive oxygen species. Science. 2013; 339:1210–1213. [PubMed: 23471409]

Martinvalet D, Dykxhoorn DM, Ferrini R, Lieberman J. Granzyme A cleaves a mitochondrial complex I protein to initiate caspase-independent cell death. Cell. 2008; 133:681–692. [PubMed: 18485875]

Martinvalet D, Zhu P, Lieberman J. Granzyme A induces caspase-independent mitochondrial damage, a required first step for apoptosis. Immunity. 2005; 22:355–370. [PubMed: 15780992]

Pitabut N, Mahasirimongkol S, Yanai H, Ridruechai C, Sakurada S, Dhepakson P, Kantipong P, Piyaworawong S, Moolphate S, Hansudewechakul C, et al. Decreased plasma granulysin and increased interferon-gamma concentrations in patients with newly diagnosed and relapsed tuberculosis. Microbiol Immunol. 2011; 55:565–573. [PubMed: 21545511]

Ricci JE, Munoz-Pinedo C, Fitzgerald P, Bailly-Maitre B, Perkins GA, Yadava N, Scheffler IE, Ellisman MH, Green DR. Disruption of mitochondrial function during apoptosis is mediated by caspase cleavage of the p75 subunit of complex I of the electron transport chain. Cell. 2004; 117:773–786. [PubMed: 15186778]

Seaver LC, Imlay JA. Alkyl hydroperoxide reductase is the primary scavenger of endogenous hydrogen peroxide in Escherichia coli. J Bacteriol. 2001; 183:7173–7181. [PubMed: 11717276]

Spaeny-Dekking EH, Hanna WL, Wolbink AM, Wever PC, Kummer JA, Swaak AJ, Middeldorp JM, Huisman HG, Froelich CJ, Hack CE. Extracellular granzymes A and B in humans: detection of native species during CTL responses in vitro and in vivo. J Immunol. 1998; 160:3610–3616. [PubMed: 9531325]

Spehr V, Schlitt A, Scheide D, Guenebaut V, Friedrich T. Overexpression of the Escherichia coli nuo-operon and isolation of the overproduced NADH:ubiquinone oxidoreductase (complex I). Biochemistry. 1999; 38:16261–16267. [PubMed: 10587449]

Steinwede K, Maus R, Bohling J, Voedisch S, Braun A, Ochs M, Schmiedl A, Langer F, Gauthier F, Roes J, et al. Cathepsin G and neutrophil elastase contribute to lung-protective immunity against mycobacterial infections in mice. J Immunol. 2012; 188:4476–4487. [PubMed: 22461690]

Stenger S, Hanson DA, Teitelbaum R, Dewan P, Niazi KR, Froelich CJ, Ganz T, Thoma-Uszynski S, Melian A, Bogdan C, et al. An antimicrobial activity of cytolytic T cells mediated by granulysin. Science. 1998; 282:121–125. [PubMed: 9756476]

Taiwo FA. Mechanism of tiron as scavenger of superoxide ions and free electrons. J Spectroscopy. 2008; 22:491–498.

Thiery J, Walch M, Jensen DK, Martinvalet D, Lieberman J. Isolation of cytotoxic T cell and NK granules and purification of their effector proteins. Curr Prot Cell Biol / editorial board, Juan S Bonifacino. 2010; Chapter 3(Unit3):37. et al.

Thoma-Uszynski S, Stenger S, Modlin RL. CTL-mediated killing of intracellular Mycobacterium tuberculosis is independent of target cell nuclear apoptosis. J Immunol. 2000; 165:5773–5779. [PubMed: 11067936]

Walch M, Rampini SK, Stoeckli I, Latinovic-Golic S, Dumrese C, Sundstrom H, Vogetseder A, Marino J, Glauser DL, van den Broek M, et al. Involvement of CD252 (CD134L) and IL-2 in the expression of cytotoxic proteins in bacterial- or viral-activated human T cells. J Immunol. 2009; 182:7569–7579. [PubMed: 19494280]

Zhao H, Kalivendi S, Zhang H, Joseph J, Nithipatikom K, Vasquez-Vivar J, Kalyanaraman B. Superoxide reacts with hydroethidine but forms a fluorescent product that is distinctly different from ethidium: potential implications in intracellular fluorescence detection of superoxide. Free Rad Biol Med. 2003; 34:1359–1368. [PubMed: 12757846]

Highlights

- Granulysin delivery of granzymes into bacteria causes their rapid death
- Granzymes target bacterial complex I to generate ROS as they do in mitochondria
- Granzymes inactivate the bacterial oxidative stress response to ensure death
- A granulysin transgene protects mice from listeria infection

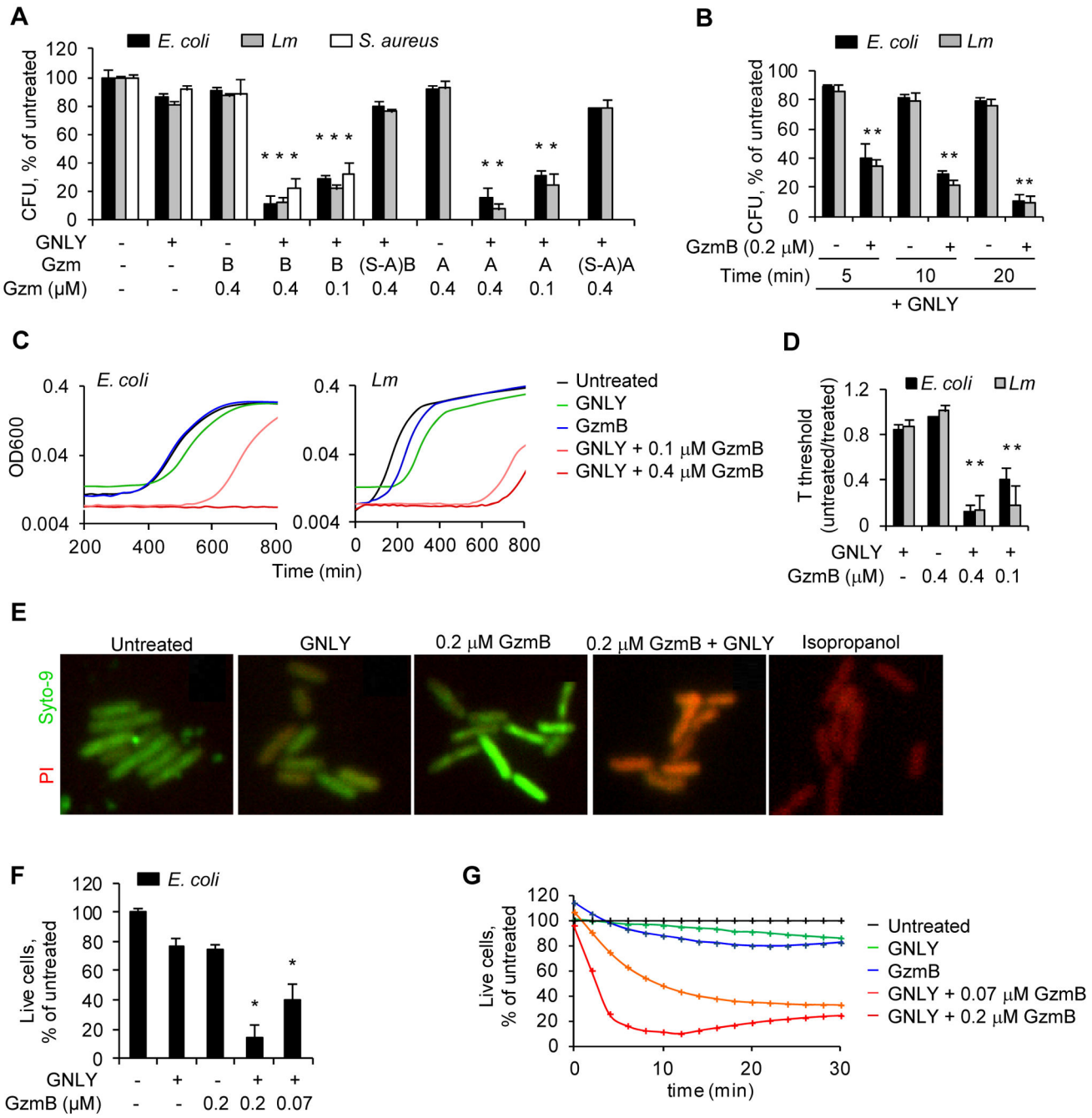

Fig. 1. Gzms and sublytic GNLY induce rapid bacterial death

(A-D) *E. coli*, *Lm* and *S. aureus* were treated with Gzms in indicated concentrations and sublytic GNLY for 20 min or indicated times before samples were harvested and bacterial viability was assessed by CFU assay (A and B), or by monitoring bacterial growth curves by optical density (C and D). For growth curves, the time to reach OD_{600} 0.05 was defined as $T_{threshold}$ (E). (S-A) refers to the Ser-Ala active site mutant inactive Gzm. (In (A), *S. aureus* was tested only for GzmB susceptibility.)

(E-G) Bacterial viability was assessed by LIVE/DEAD® assay after incubation with sublytic GNLY and GzmB in the indicated concentrations and times. Syto-9 enters live and dead bacteria, while PI only enters dead bacteria. (E) shows representative staining of *E. coli* treated as indicated for 20 min and (F) is the quantification of live cells relative to untreated bacteria. (G) shows a representative time course.

Bar graphs show the mean±SEM of at least 3 independent experiments; in other panels representative data from at least 3 experiments are shown. Statistical differences compared to untreated control samples were calculated using unpaired Student's t-test. *, $P<0.05$.

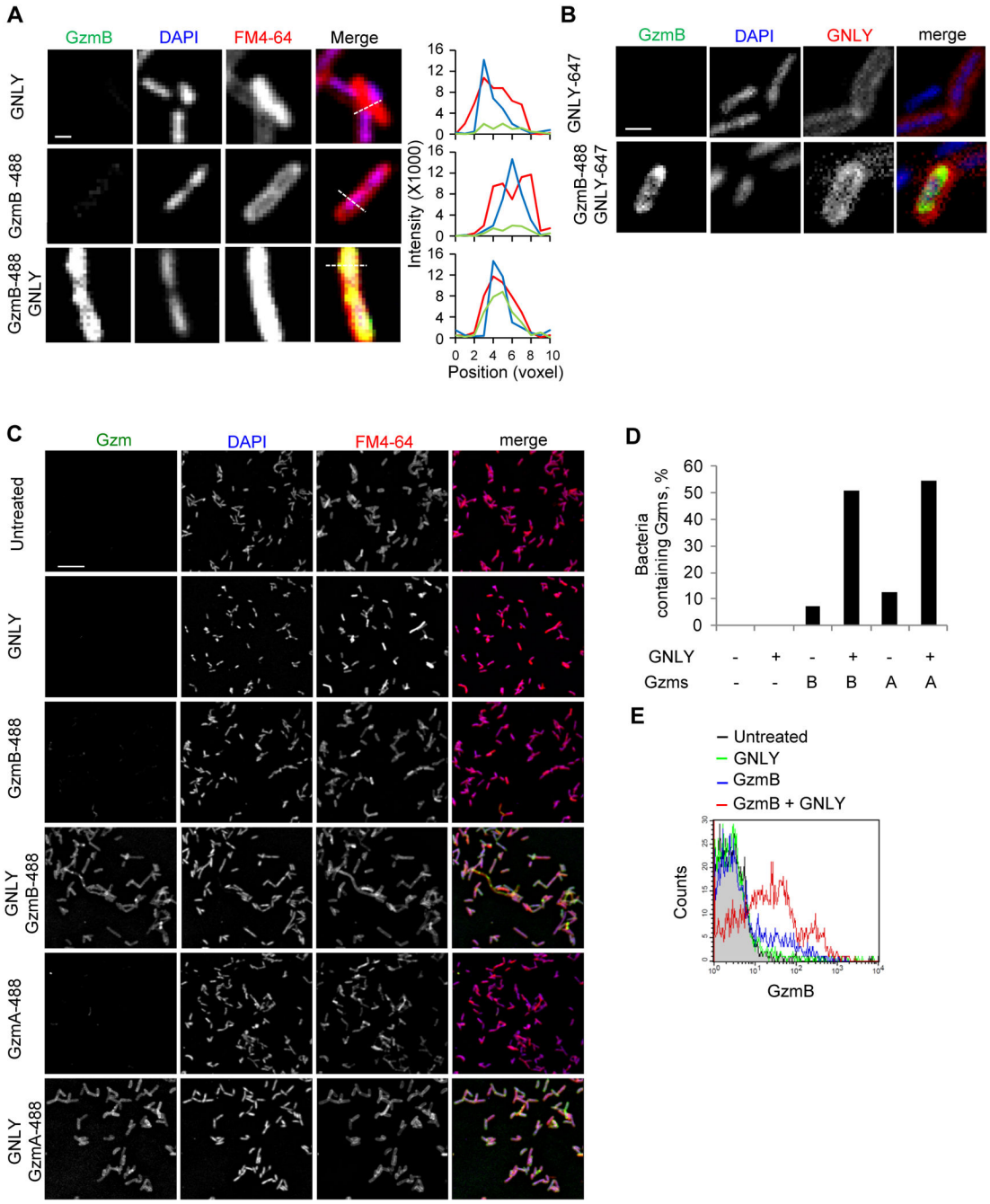

Fig. 2. Sublytic GNLY delivers Gzms into bacteria

(A-C) *E. coli* treated with catalytically inactive, AF488-labeled GzmB (GzmB-488) ± sublytic unconjugated (A and C) or AF647-conjugated GNLY peptide (B), were stained with FM4-64 and DAPI and visualized by confocal microscopy. High resolution images (A and B) and representative fields are shown (C). Fluorescence intensity for each color in (A) was measured along the indicated dashed lines. Bars, 1 μm (A and B) and 10 μm (C).

(D) Analysis of the percentage of bacteria in which GzmB clearly localized within bacteria based on counting 400-3000 bacteria per condition. Representative 3-dimensional images are in Supplemental movies 1-6

(E) *E. coli*, treated with inactive GzmB ± sublytic GNLY, were stained with anti-GzmB and analyzed by flow cytometry.

Experiments in panels (A-C and E) are representative of at least 3 independent experiments.

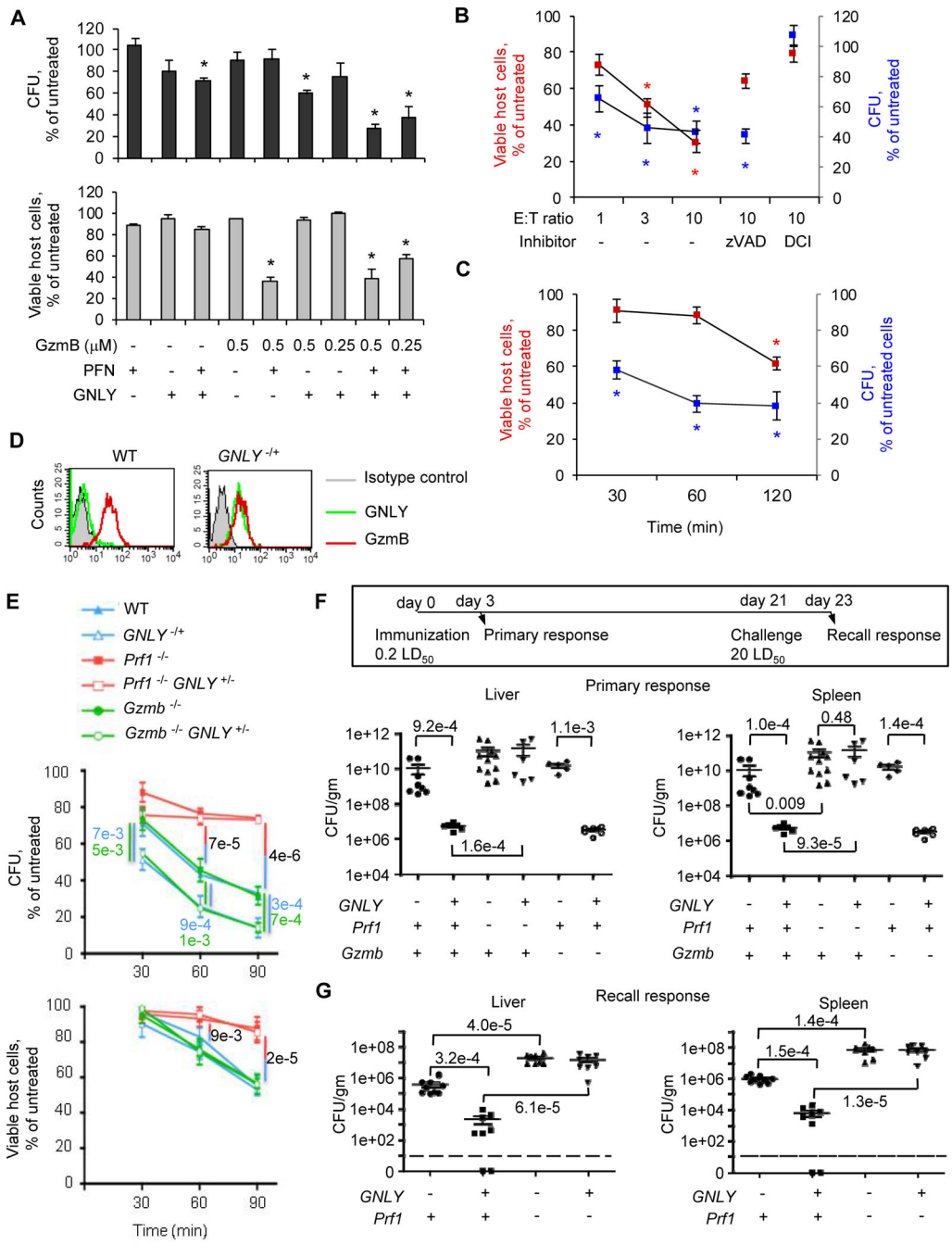

Fig. 3. Intracellular *Lm* are killed in a Gzm, GNLY and PFN-dependent process

(A) *Lm*-infected HeLa cells were treated with GzmB, PFN and/or GNLY in indicated concentrations and analyzed 1 hr later for bacterial CFU (upper) and host cell viability by Annexin V-PI staining (lower).

(B and C) *Lm*-infected MDDC were incubated for 2 hr with human *Lm*-specific CTLs at indicated E:T ratios in (B) or at an E:T ratio of 3 for indicated times in (C) before assessing host cell viability by ^{51}Cr-release and intracellular bacterial CFU. In (B) experiments were

performed in the absence of inhibitors or in target cells treated with zVAD-fmk or by using effector cells pretreated with the Gzm inhibitor DCI.

(A-C) show mean±SEM of 3 independent experiments; asterisks indicate statistically significant differences ($P<0.05$) compared to untreated cells by unpaired Student's t-test.

(D and E) Splenocytes from WT or *GNLY*-Tg BALB/c mice were stimulated with IL-2 *in vitro* for 5 d before evaluating GNLY and GzmB levels by flow cytometry (D). Splenocytes from *Lm*-primed WT or GNLY-Tg mice in WT, *Prf1*$^{-/-}$ or *Gzmb*$^{-/-}$ backgrounds were isolated 8 d post-infection and then cultured for indicated times at an E:T ratio of 3 with *Lm*-infected RAW264.7 cells coated with anti-CD3. Viable bacteria in hypotonically lysed cells were assessed by CFU assay (E, top) and host cell viability was measured in parallel by ^{51}Cr-release. (E, bottom). Statistically significant P values calculated by unpaired Student's t-test between cells from WT and *GNLY*-Tg mice in each background are shown.

(F) For the primary response, WT, *GNLY*-Tg, *Prf1*$^{-/-}$, *Prf1*$^{-/-}$*GNLY*-Tg, *GzmB* $^{-/-}$ and *GzmB* $^{-/-}$*GNLY*-Tg BALB/c mice were infected i.p. with 0.2 LD_{50} *Lm*, and bacterial counts in the spleen and liver were measured 72 hr later.

(G) For the recall response, WT, *GNLY*-Tg, *Prf1*$^{-/-}$, and *Prf1*$^{-/-}$*GNLY*-Tg BALB/c mice were immunized i.p. with 0.2 LD_{50} *Lm* and 3 wk later challenged i.p. with 20 LD_{50}. Bacterial counts in the spleen and liver were measured 40 hr later. Black bars show mean log-transformed colony counts. Dashed lines indicate the detection limit.

Statistical differences compared to WT mice or between WT and *GNLY*-Tg mice in each background were calculated using the Wilcoxon rank-sum test; significant P values are shown.

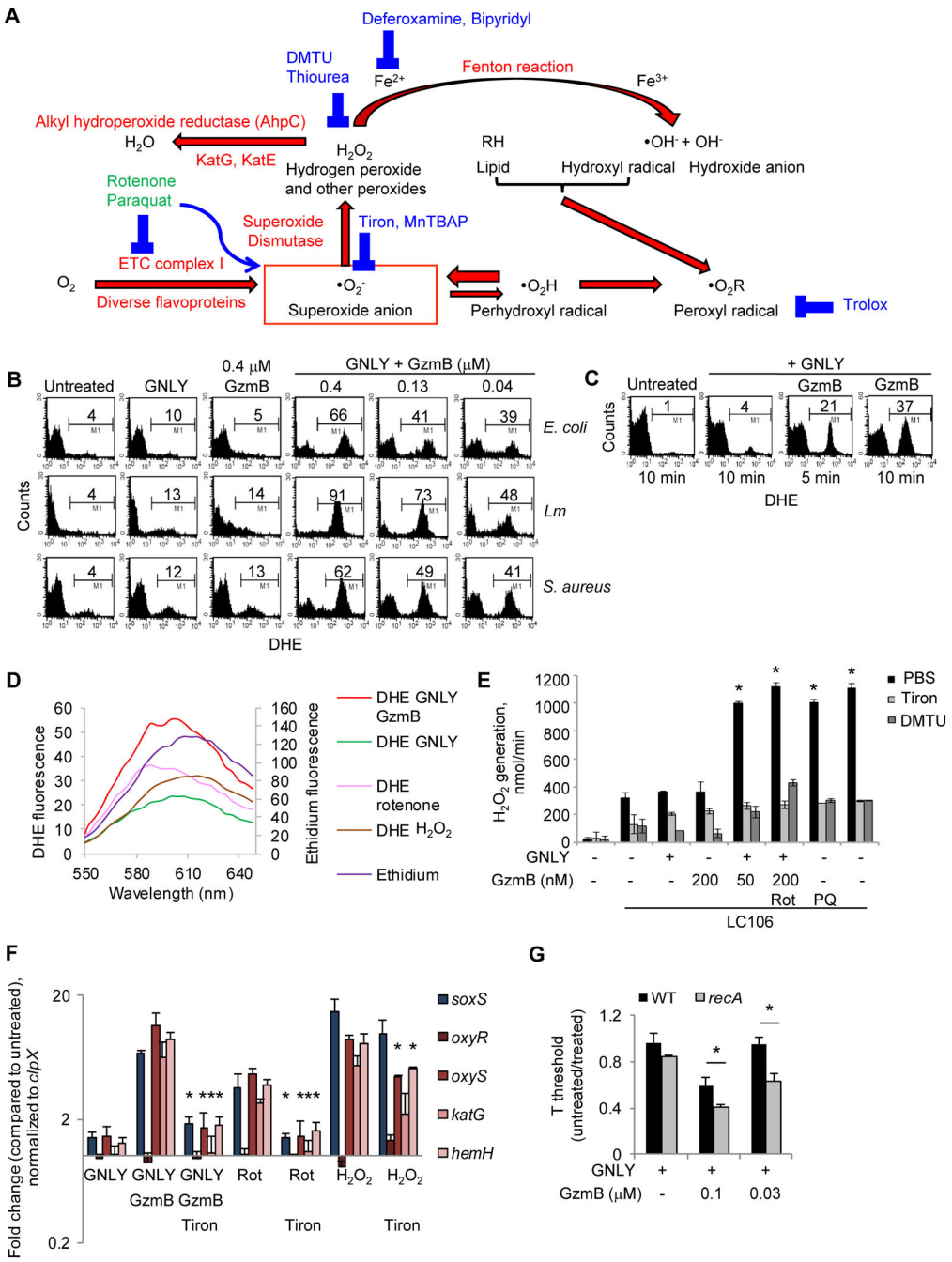

Fig. 4. Gzms rapidly induce ROS in bacteria

(A) Schematic of ROS production and metabolism in *E. coli*. ROS scavengers (blue) and superoxide inducing poisons (green) act at the indicated sites.

(B) Bacteria treated for 20 min with GzmB in indicated μM concentrations ± sublytic GNLY were stained with the fluorescent superoxide reporter, dihyroethidium (DHE) and assayed by flow cytometry.

(C) Time course of DHE staining after treatment with sublytic GNLY and 200 nM GzmB. (B and C) show representative data from 3 independent experiments.

(D) *E. coli* were treated with 150 nM GzmB + sublytic GNLY, GNLY only, rotenone, H_2O_2 or left untreated for 10 min and stained with DHE or ethidium before scanning fluorescent emission spectra (excitation at 488 nm).
(E) Catalase/peroxidase-null *E. coli* strain LC106 was treated for 15 min with 200 nM GzmB ± sublytic GNLY, rotenone (rot, 20 μM) or paraquat (PQ, 200 μM) in the presence or absence of Tiron or DMTU before the reaction was diluted in PBS containing Amplex Red/horseradish peroxidase. H_2O_2 production was measured by the increase in Amplex Red fluorescence. Mean±SEM of 3 independent experiments is shown. Statistically significant differences ($P<0.05$) compared to untreated cells, calculated by unpaired Student's t-test, are indicated by asterisks.
(F) Oxidative stress-regulated RNAs were analyzed by quantitative RT-PCR in *E. coli* treated for 10 min with 150 nM GzmB ± GNLY, rotenone (10 μM) or H_2O_2 (40 μM) in the presence or absence of 10 mM Tiron. Mean±SEM of 5 independent experiments is shown. Statistically significant differences ($P<0.05$), compared to corresponding samples without Tiron, were calculated by unpaired Student's t-test and are indicated by asterisks.
(G) *recA*-deficient *E. coli* or the parental strain (ML1655) were treated with indicated concentrations of GzmB ± GNLY for 15 min and viability was assessed by bacterial growth. The time to reach OD_{600} 0.05 was defined as $T_{threshold}$. Mean±SEM of 3 independent experiments is shown. Significant differences compared to WT bacteria, calculated using unpaired Student's t-test, are indicated by asterisks. *, $P<0.05$.

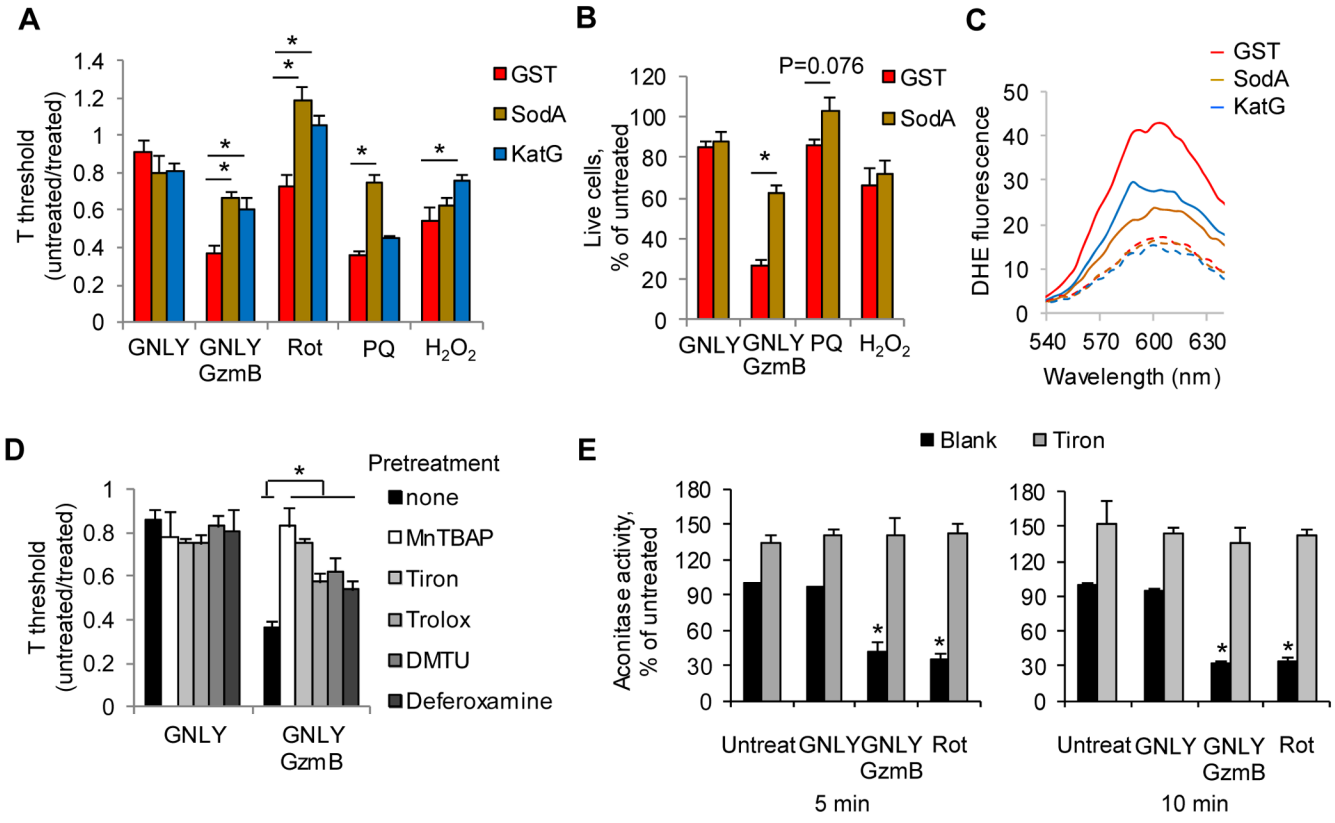

Fig. 5. ROS contribute to rapid bacterial death induced by the granzymes

(A) *E. coli* overexpressing SodA, KatG or GST were treated for 15 min with 150 nM GzmB ± GNLY, rotenone (Rot, 10 μM), paraquat (PQ, 100 μM) or H_2O_2 (200 μM) and analyzed for bacterial growth.

(B) *E. coli* overexpressing *sodA* or *GST* as control were treated with 150 nM GzmB ± sublytic GNLY, GNLY only, paraquat (PQ, 500 μM) or hydrogen peroxide (H_2O_2, 500 μM) for 15 min and analyzed by LIVE/DEAD® assay.

(C) *E. coli* overexpressing superoxide dismutase (SodA), catalase (KatG) or empty vector (GST) were treated with 150 nM GzmB + sublytic GNLY or left untreated for 10 min and stained with DHE before scanning the fluorescent emission spectra after excitation at 488 nm. Solid lines indicate GNLY/GzmB-treated bacteria; dashed lines are control untreated bacteria.

(D) *E. coli* were incubated with ROS scavengers MnTBAP, Tiron, Trolox, Dimethylthiourea (DMTU) or the iron-chelator, deferoxamine, and treated with 150 nM GzmB ± GNLY for 15 min before assessing bacterial growth. The sites of action of SOD, catalase and the chemical ROS scavengers are shown in Fig. 4A. Graphs in (A, B, D) show the mean±SEM of at least 3 independent experiments. Statistical differences, calculated relative to GST control or untreated samples using unpaired Student's t-test, are indicated by asterisks. *, $P<0.05$.

(E) *E. coli* treated with 400 nM GzmB and sublytic GNLY or 2.5 μM rotenone in the absence or presence of 20 mM Tiron for indicated times were lysed and aconitase activity in the cleared bacteria lysates was measured. Data were normalized to untreated bacteria in the

absence of Tiron. Graphs show the mean±SEM of 3 independent experiments. Significant differences compared to untreated control samples, calculated using unpaired Student's t-test, are indicated by asterisks. *, $P<0.05$.

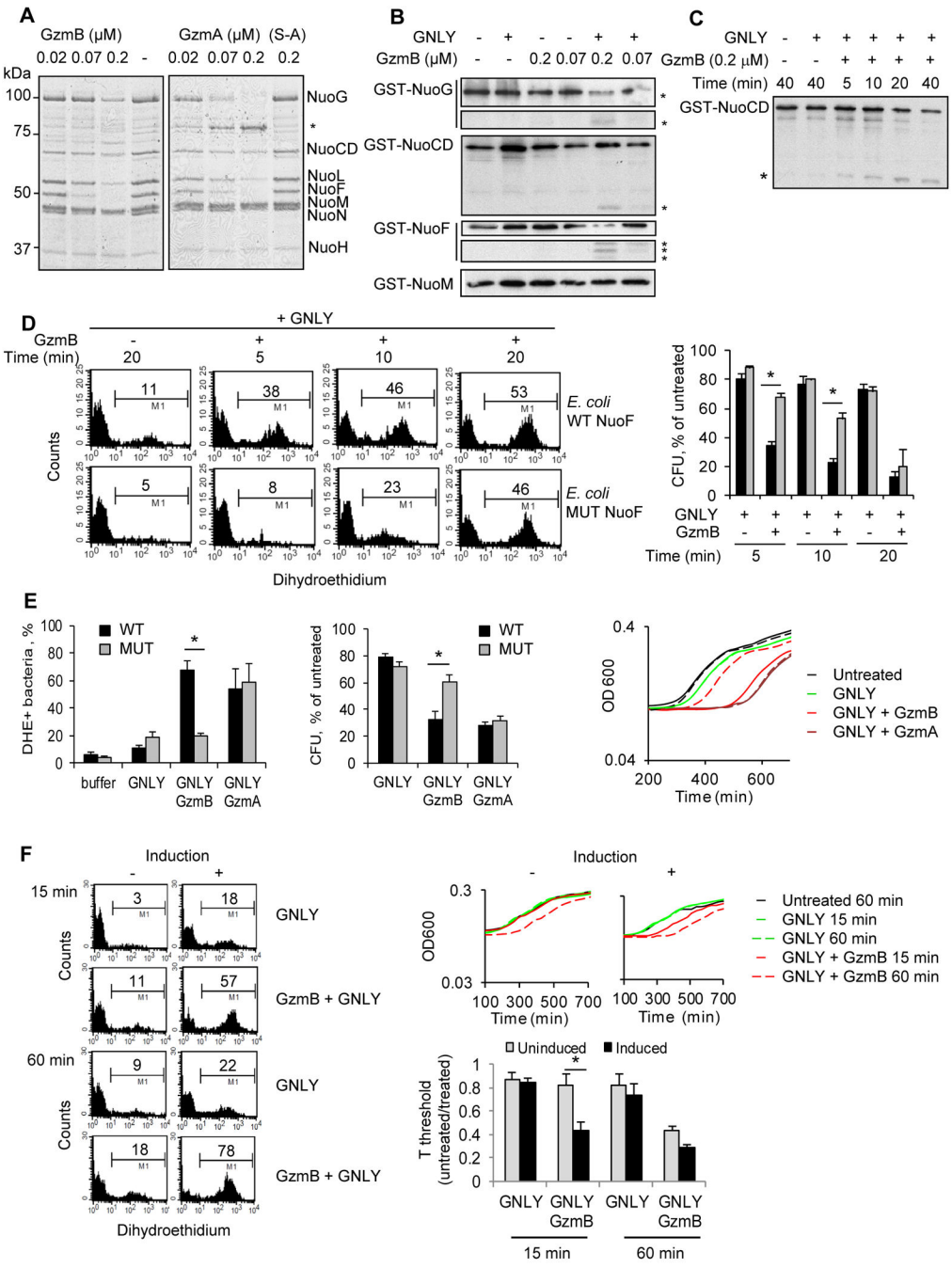

Fig. 6. Gzms cleave complex I subunits to cause oxidative damage

(A) Purified *E. coli* complex I was treated with GzmA (or its inactive mutant (S-A)) or GzmB in indicated concentrations for 10 min before SDS-PAGE and Coomassie staining. The **N**ADH:**u**biquinone **o**xidoreductase (Nuo) subdomains corresponding to each visible band are labeled. * indicates a NuoG GzmA cleavage fragment.

(B) *E. coli* expressing GST-tagged NuoCD, NuoF, NuoG or NuoM were treated with sublytic GNLY and/or GzmB for 20 min. GST immunoblots are shown; * indicates cleavage fragments.

(C) The kinetics of NuoCD cleavage in *E. coli*.

(D) *E. coli* overexpressing wild-type (WT) or GzmB-uncleavable mutant (MUT) NuoF were treated with GNLY and GzmB for indicated times before measuring ROS by flow cytometry (left) or bacterial viability by CFU assay (right).

(E) *E. coli* overexpressing WT or MUT NuoF were treated with GNLY and GzmB or GzmA for 10 min before assessing ROS by DHE fluorescence (left) and viability by CFU assay (middle) or growth curves (right; solid lines, bacteria expressing WT NuoF; dashed lines, bacteria expressing MUT NuoF). Statistically significant differences ($P<0.05$) between WT and MUT strains are indicated.

(F) *E. coli* strain ANN0221/*pBADnuo/His-nuoF* expressing inducible complex I was induced or not for 60 min with L-arabinose before treatment with GNLY ± GzmB for 15 or 60 min. ROS production was measured by DHE staining and flow cytometry (left) and bacterial viability was assessed by bacterial growth curves (right).

Representative flow cytometry histograms and growth curves and mean±SEM of at least 3 independent experiments are shown. Significant differences ($P<0.05$) between indicated groups, calculated using unpaired Student's t-test, are indicated by asterisks.

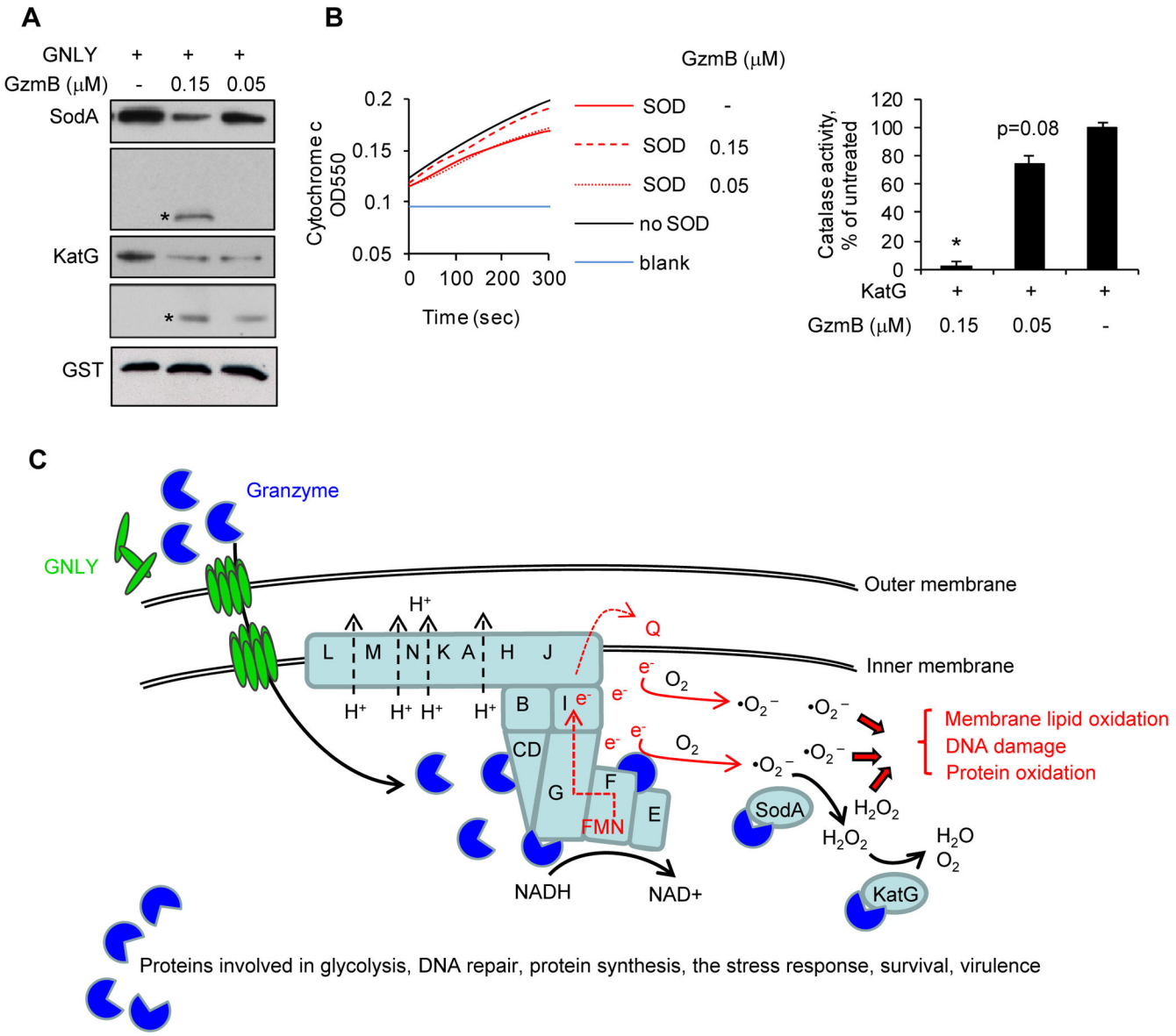

Fig. 7. Granzyme destroys ROS degrading enzymes and model of GNLY/GzmB induced bacterial death

(A) *E. coli* expressing GST-SOD (*SodA*), GST-catalase (*KatG*) or empty vector (GST) were treated with GzmB and sublytic GNLY for 20 min. Cleavage was assessed by GST immunoblot. Cleavage products are indicated by asterisks.

(B) Purified GST-SodA (20 nM, left) or GST-KatG (1 μM, right) were pretreated for 20 min with indicated concentrations of GzmB before assessing enzyme activity. SOD activity was assessed by measuring cytochrome c reduction. Catalase activity relative to GzmB-untreated samples was assessed by oxidation of phenol red in the presence of horseradish peroxidase. Representative curves (left) or mean±SEM of 3 independent measurements (right) are shown. Significant differences compared to untreated control samples, calculated using unpaired Student's t-test, are indicated by asterisks. *, P<0.05.

(C) Model for GzmB/GNLY action on bacteria. GNLY permeabilizes bacterial membranes to allow Gzms to enter the bacterial cytosol, where they attack catalytic subunits of ETC complex I. Cleavage of ETC complex I interferes with transport of electrons, which leak into the cytosol to reduce oxygen to superoxide. Sod and catalase are also cleaved to prevent detoxification of superoxide anion. Increased ROS lead to membrane, protein and DNA damage. Cleavage of other bacterial proteins also contributes to bacterial death.